INVESTIGATION OF THEORETICAL PERFORMANCE OF THE VORTEX TUBE

G.M.Harish[#1], B.B.Hariram[#2], R.Dilipkumar[#3], M.Gokul[#4], Mr.N.R.Karthik[#5], Mr.K.Karthikeyan[#6]

#1, 2/214-A, S.V.Nagar, P.N.Pudur Post, Coimbatore-641 041, Ph: 9751597170.

#2, 4/43, 2nd street, Sundhar Nagar, Paramakudi, Ramanadhapuram-641 707, Ph: 8220624271.

#3, 6/183 D, Kaveri Nagar, Pattanam, Coimbatore-641 016, Ph: 9943084118.

#4, 12/39, Kambaliyampatti (po), Sangarandam palayam (via), Kangeyam (Tk), Tirpur-638 706, Ph: 9159071909.

#5, Assistant Professor, Department of Mechanical Engineering, Sri Ramakrishna Engineering College, Vattamalaipalayam, NGGO Colony (Po), Coimbatore-641 022. Ph: 9578578979.

#6, Assistant Professor, Department of Mechanical Engineering, Sri Ramakrishna Engineering College, Vattamalaipalayam, NGGO Colony (Po), Coimbatore-641 022. Ph: 984229341.

1. ABSTRACT

In this paper we studied the performance of the vortex tube at various pressures and cold mass fractions. The experimental results of the cold end temperature drop were taken from [9]. The pressure was varied from 3 bar to 5 bar whereas the cold mass fraction was varied from 20% to 90%. The COP and the Refrigeration effect of the vortex tube were calculated from the results available theoretically by using a reciprocating air compressor of specification as shown in Table 1 and the results were studied. Further, the temperature drop of different working media (air, nitrogen and carbon dioxide) are also taken from [9] and studied.

2. INTRODUCTION

A vortex tube is a simple-structure device which can separate a compressed stream into a hot and a cold stream. The generation of separated cold and hot streams from a single injection in a vortex tube is known as the Ranque effect. The accurate flow pattern inside the vortex tube remains elusive and no satisfactory explanation of its energy separation mechanism has been put forward yet. A typical vortex tube is shown in Figure 1.
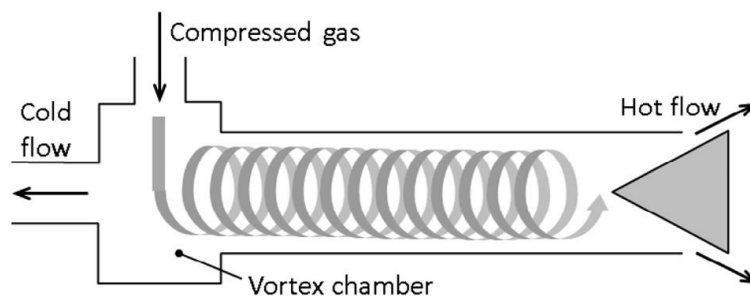
Figure1. Typical Vortex Tube

Ranque–Hilsch vortex tube having, relatively simple geometry, no moving mechanical parts and no need for absolute sealing element, was invented by Ranque [21] demonstrating the effect of temperature separation of gases. Later, Hilsch [22] described this effect in detail. Intensive experimental and analytical studies of Ranque–Hilsch effect began since then and continue even today. According to these studies when a vortex tube is injected with compressed gas through tangential nozzles into its scroll chamber, a strong circular flow field is established. This vortex in the inlet area causes pressure distribution of the flow in radial direction. As a result a free vortex is produced as the peripheral warm stream and a forced vortex as the inner cold stream. The flow pattern is schematically shown in Figure 2. The tangential velocity of the fluid element is related to the distance r from the axis of rotation as, v / r, for forced vortex or quasi-solid rotation and v / 1/r, for free vortex or potential vortex. The variation of tangential velocity along the radius for such a case in a vortex tube representing forced region and free region is shown in Figure 3. Many investigators, Hilsch [22], Deissler and Perlmutter [23], Kurosaka et al. [24], Ahlborn et al. [25], Cockerill [26], Gutsol [27], have suggested various theories to explain the Ranque effect. Ahlborn et al. [28] have postulated a theory of temperature separation based on heat pump mechanism enabled by secondary circulation flow in vortex tubes. However till today no exact theory has come up to explain the phenomenon satisfactorily. Thus much of the design and development of vortex tubes have been based on empirical correlations leaving much scope for optimization of critical parameters. Computational fluid dynamics techniques have revolutionized engineering design in several important areas, notably in analysis of fluid flow technology. CFD can also be used as a minimal adequate tool for design of engineering components.

As we reviewed the literature, there were no numerical analyses to investigate the effects of gas type on the performance of the vortex tube. There was no comprehensive numerical work for studying the effect of vortex tube diameter; most were experiments. One, who undertook his work numerically, just investigated two different diameters and concluded that vortex tubes have a better performance with smaller diameters. We do not believe this is sufficient, so in the present work, different diameters have been used for studying in depth. In the present work, different gases were used as a refrigerant in a vortex tube, to understand which one produces maximum cooling temperature differences.
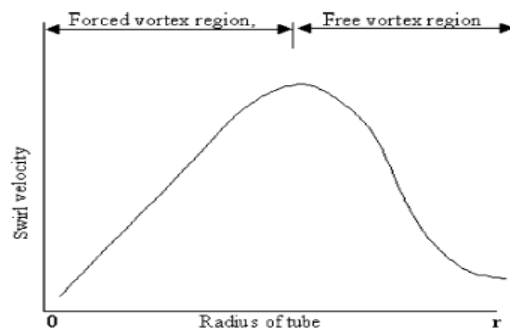
**Figure 2. Schematic Velocity Distribution in Ranque–Hilsch Vortex Tube**
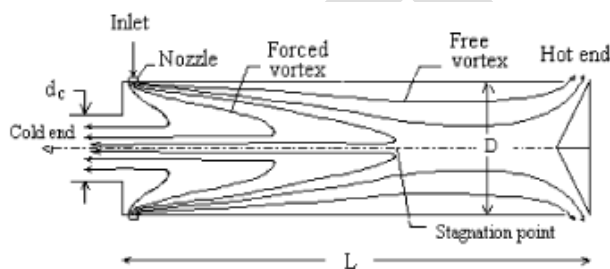
Figure 3. Schematic Flow Pattern of Ranque–Hilsch Vortex Tube

To do this, helium, air, nitrogen, oxygen, carbon dioxide, ammonia and water were selected. Also, the effects of varying the geometry of vortex tube components, such as hot outlet and diameter size, on tube performance, have been studied.
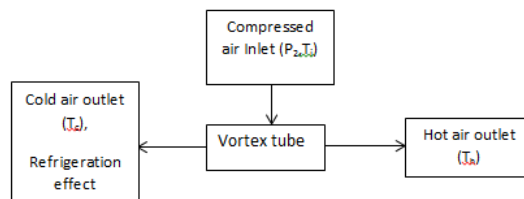
3. EXPERIMENTAL SETUP
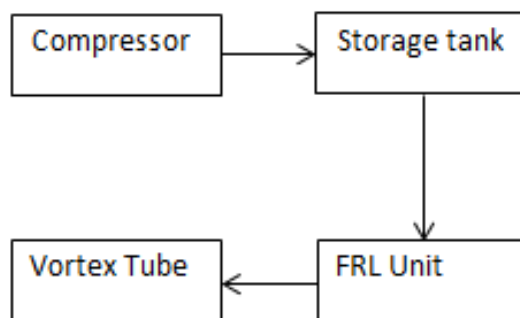
Figure 4. Block Diagram Of Experimental setup
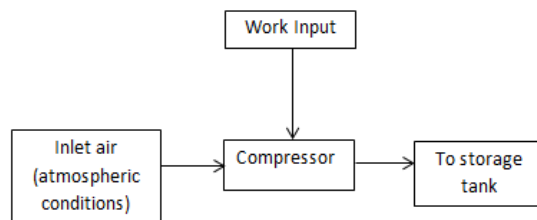
Figure 5. Block Diagram Of Compressor

Figure 6. Block Diagram Of Vortex Tube

A contour flow type RHVT of Saidi and Valipour [20] has been employed in this study. Compressed gas (air) is provided by air compressor [1] and is set at a fix pressure by means of pressure regulator. Pressurized air passes the inlet valve [2] and filter section [3]. The working fluid (air) is introduced tangentially into the vortex tube [7] producing two swirling flows. Both swirling flows generate high rotating vortex motion. One is the peripheral swirling flow that swirls to the hot end and the other is anti-swirls to the cold end known as a central swirling flow. The cold stream flows out of the tube through cold orifice while the hot stream leaves the tube through the hot exit. The control valve (needle valve) may control the flow rate of the hot air [12]. The experimental results of the cold end temperature drop at different mass fractions were taken from [9] and the theoretical analysis such as COP analysis and Refrigeration effect analysis were done by using a compressor having specifications as shown in Table 1.

4. TERMINOLOGIES AND FORMULAE

TERMINILOGIES

P_1 = Inlet pressure to compressor
P_2 = Outlet pressure from compressor
V_1 **=** Total volume
V_3 = Clearance volume
V_S **=** Swept volume
$V_1 - V_4$ = Swept volume
V_d = Discharge volume
η_v = Volumetric Efficiency
FAD   = Free air delivered
C   = Clearance Ratio
D   = Bore Diameter of cylinder
L   = Length of the stroke
N   = Speed (in RPM)
m   = Mass flow rate (kg/s)

ΔT =Temperature Difference of cold end and hot end
C_p = Specific heat capacity
R   = Gas constant
Q   = Refrigeration effect for vortex tube
W   = Work done by compressor

FORMULAE

W $= (n/n\text{-}1)*P_1 V_{S*}[(P_2/P_1)^{(n\text{-}1)/n}\text{-}1]$
COP   = Q/W
m $= (P_1 * FAD)/ (R * T_1)$
FAD $= \eta_v * V_d$
η_v $= 1 - C\,[(P_2/P_1)^{1/n} -1]$
R   = 0.287 kJ/kg k
C $= V_c/V_s$
V_c $= C* V_s$
V_d $= (V_1 * N)/60$
V_s $= (\pi/4)*D^2*L$
V_1 $= V_c + V_s$
V_3 $= V_s * 0.05$
V_4 $= 2.69 * V_3$
$V_4/V_3 = (P_2/P_1)$
Q $= m\, C_p\, \Delta T$
C_p = 1.005 kJ/kgK

COMPRESSOR SPECIFICATION

Bore diameter	0.085 m
Stroke length	0.0889 m
Speed	750 rpm

Table 1. Compressor Specification

5. GOVERNING EQUATION

The flow inside the vortex tube of dry air is assumed to be compressible, accompanied by strong swirling, three-dimensional, and in steady state in developing the governing equations. The special flow condition that may result in very low temperature makes the working fluid (dry air) departure significantly from the perfect gas behavior. Hence, the use of real gas model is necessary for the numerical calculation. According to the description of the physical model of the vortex tube, the governing equations including the continuity equation, momentum conservation equation, and energy conservation equation [15] are listed below.

Continuity equation

$$\nabla \cdot (\rho \vec{v}) = 0$$

Momentum conservation equation

$$\nabla \cdot (\rho \vec{v} \vec{v}) = -\nabla p + \rho \vec{g} + \nabla \cdot \bar{\bar{\tau}} + \vec{F}$$

Energy conservation equation

$$\nabla \cdot [\vec{v}(\rho E + p)] = \nabla \cdot (k_e \nabla T + \bar{\bar{\tau}} \cdot \vec{v}) + S_h$$

Where r, E, v, p, and T is air density, volumetric total energy, velocity
vector static pressure, and static temperature, respectively. Pg is gravitational body force, F
vector is external body forces. Ke is effective conductivity, and Sh includes other volumetric
heat sources we must defined. ρE is total energy and is given by

$$\rho E = \rho e + \frac{1}{2}\rho(\vec{v} \cdot \vec{v}) \quad e = c_v T$$

e is internal energy. τ is stress tensor and is expressed as follows,

$$\bar{\bar{\tau}} = \mu \left[\left(\nabla \vec{v} + \vec{v}^T \right) - \frac{2}{3} \nabla \cdot \vec{v} I \right]$$

Where, m is air molecular viscosity, I is unit tensor, and the second term on the right
hand side is the effect of volume dilation.
For the compressible flows, the equation of state (EOS) is needed for relating pressure, volume
and temperature. Redliche-Kwong Equation [19] is used here considering the fact that the air
pressure is not very high and temperature is not very low,

$$p = \frac{RT}{V - b_1} - \frac{a_1}{T^{1/2}V(V + b_1)}$$

where, R is gas constant, a1 and b1 are defined by,

$$a_1 = 0.42748 \frac{R^2 T_{cr}^{2.5}}{p_{cr}}$$

$$b_1 = 0.08664 \frac{RT_{cr}}{p_{cr}}$$

where,
P_{cr} = Critical pressure (Pa)
T_{cr} = Critical temperature (K).

6. BOUNDARY CONDITION

The inlet pressure to the vortex tube is varied from 3 bar to 5 bar and cold mass fraction is varied from 20% to 90% by adjusting the hot end plug. The cold fluid mass fraction [10] is defined by,

$$\xi = \frac{\dot{m}_c}{\dot{m}_i}$$

where ,
m_c = The mass flow rate of the cold fluid(kg/s)
m_i = The total inlet mass flow rate of the working fluid (kg/s)
The boundary conditions and the main operation parameters are listed in table 2.

INLET PRESSURE (kN/m^2)	INLET TEMPERATURE (K)	MASS FLOW RATE(kg/s)
500	298	6.60e-5
400	298	6.77e-5
300	298	6.96e-5

Table 2. Boundary Condition

7. RESULTS AND DISCUSSIONS

Experiments are conducted on vortex tube with L/D ratio of 17.5 . Inlet pressure is also varied from3 to 5 bar in the increment of 1 bar. For the testing, cold mass fraction is varied in the range of 20% to 90% with the step size of 10%. Variation of cold end temperature drop (Ti − Tc) with the the effect of cold mass fraction is shown in Figure 8. The cold mass fraction is varied by opening the needle valve gradually. The supply pressure of air was maintained at 4 bar. It can be seen that , initially cold end temperature drop increases to maximum and attains an optimum value at a cold mass fraction of 60%. Maximum value of cold end temperature drop of 29 °C is obtained for L/D ratio 17.5 at 60% cold mass fraction. Cold stream mixes with hot stream resulting drop in cold end temperature drop. The effect of cold mass fraction on COP was also studied at (L/D) ratio of 17.5 . The cooling effect produced in the vortex tube depends on properties of the working fluids viz. molecular weight, specific heat capacity ratio and moisture content of gas. Experiments were performed with three different working fluids as air, nitrogen and CO2. Figure 7 shows the cold end temperature drop with supply pressure for chosen working media with cold mass fraction 30%. The result shows that CO2 produces higher cold end temperature drop than air and nitrogen [18]. At pressure of 4 bar cold temperature drop for CO2, -nitrogen and air are 23 °C, 18 °C and 20 °C, respectively.

The highest temperature drop is obtained with CO2 due to the higher molecular weight and lower gas constant of CO2 in comparison to other gases. Further, lower specific heat ratio (γ) of the CO2 may also contribute to get the maximum cold temperature drop for CO2. The temperature drop increases directly with pressure since higher pressure is indicative of more

work potential. However, it cannot be said with confidence that temperature drop will continue to increase at this rate beyond 5 bar pressure without more experimentation.

GAS	SPECIFIC HEAT CAPACITY RATIO (K)	MOLECULAR WEIGHT
Helium	0.1520	04.003
NH$_3$	0.0247	17.031
Water (vapour)	0.0261	18.015
Nitrogen	0.0242	28.013
Air	0.0242	28.966
Oxygen	0.0246	31.999
CO$_2$	0.0145	44.001

**Table 3. Properties Of Different Gases**

Figure 8 depicts the variation of the cold end temperature drop with cold mass fraction at various inlet pressures of air. It is shown that increasing the inlet pressure increases the cold end temperature drop up to cold mass fraction of 60%. The highest temperature drop measured is 32 °C at the inlet pressure 5 bar while 29 °C and 26 °C temperature drop were obtained at 4 bar and 3 bar pressure supply respectively. The highest cold end temperature drop at the respective operating pressures is seen at 60% cold mass fraction [9].
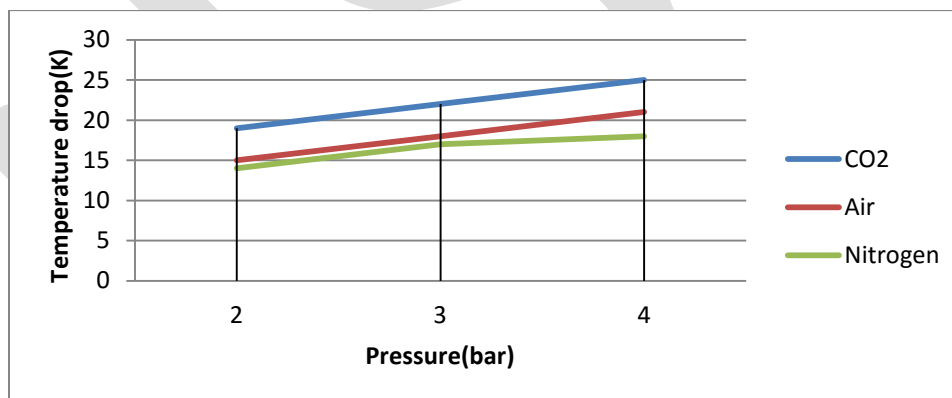

Figure 7. Temperature drop Vs Pressure

This is due to the reason that as the pressure increases it causes flow velocity to increase which become responsible for energy separation. Increase in cold mass fraction beyond 60% reduces the cold temperature drop. This can be attributed to the fact that as cold mass fraction is increased beyond this value (60%), some of the operating fluid in which energy separation as already occurred (which is at relatively higher temperature) is also drawn at cold end. This will cause mixing of hot and cold mass of working fluid leading to net reduction in cold temperature drop. Considering the fact the cold end temperature drop is at the maximum at 5 bar, it can be said that the chosen vortex tube of L/D 17.5 is capable of causing full expansion of the working

medium air at this pressure as shown in Figure 11. However, the same trend may not be continuing at higher working pressures. Further, it can be inferred that if the cold mass fraction is made 100% the working fluid temperature at the cold end would become same as its temperature at the inlet, i.e. causing the cold end temperature drop to reduce to zero.
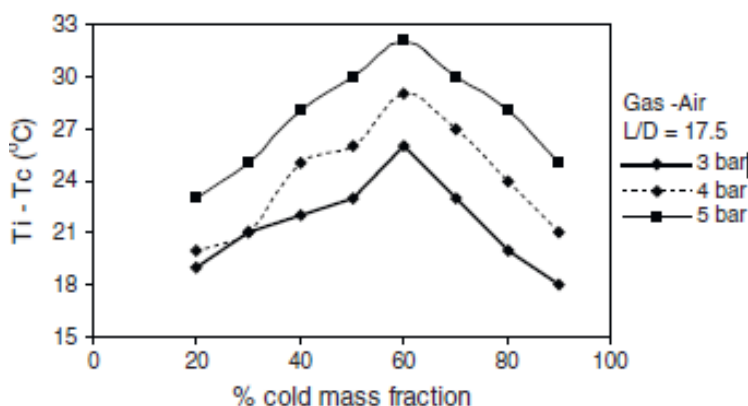
**Figure 8. Temperature drop Vs Cold mass fraction**

At a Pressure of 3 bar,4 bar,5 bar, the graph between COP and cold mass fraction is as shown in Figure 9.
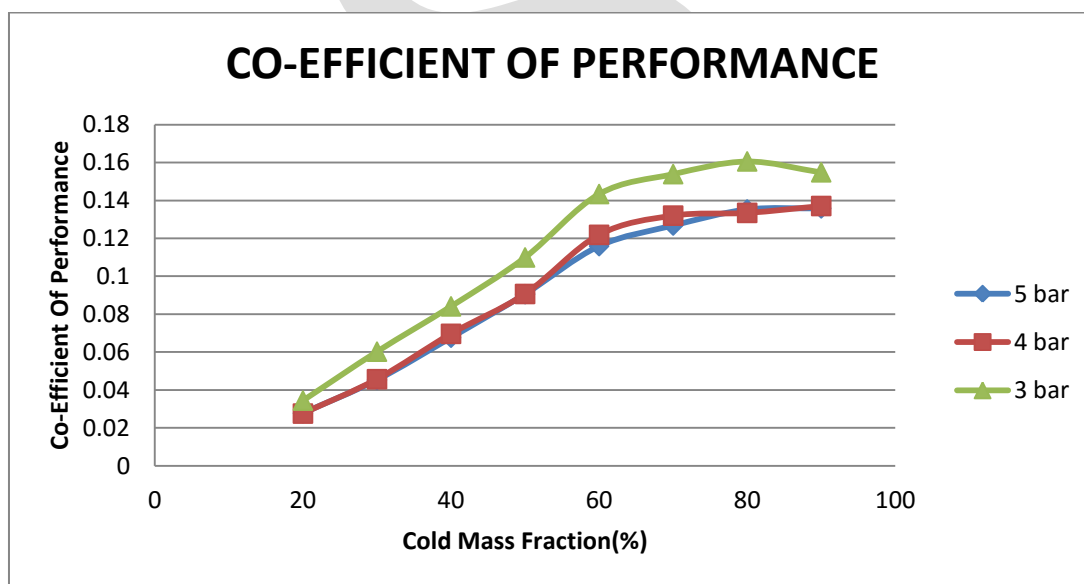
Figure 9. COP Vs Cold mass Fraction

It is found that the COP of the Vortex Tube is maximum at a cold mass fraction of 90% for pressure of 5 bar, 4 bar and at a cold mass fraction of 80% for 3 bar.
At a Pressure of 3 bar,4 bar,5 bar, the graph between Refrigeration effect and cold mass fraction is as shown in Figure 10.
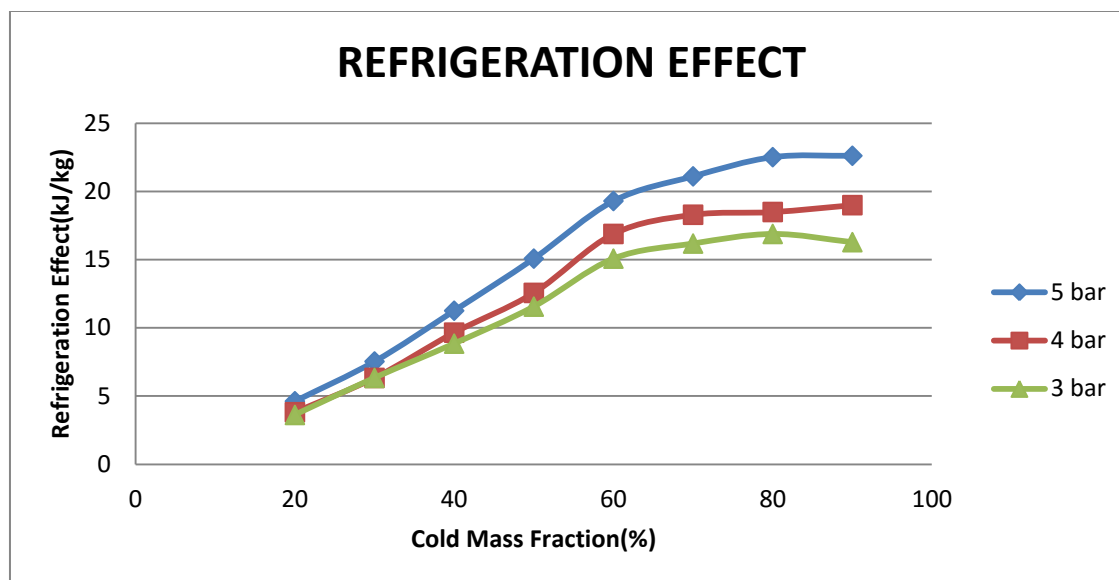
Figure 10. Refrigeration Effect Vs Cold Mass Fraction

It is found that the Refrigeration Effect of the vortex tube is maximum at a cold mass fraction of 90% for pressure of 5 bar,4 bar and at a cold mass fraction of 80% for 3 bar.

8. CONCLUSION

Performance evaluation of the Ranque–Hilsch vortex tube has been carried out theoretically . There is a value of cold mass fraction at which vortex tube has the highest temperature drop for all the given pressures at the L/D ratio of 17.5 [9]. The maximum cold end temperature drop is obtained at cold mass fraction of 60%. For the given L/D ratio, as the gas pressure increases, cold end temperature difference increases but the optimum value of cold mass fraction remains same. In the tested range, COP and Refrigeration effect increases as the cold mass fraction increases at the pressures of 4 bar and 5 bar. At a pressure of 3 bar the maximum COP and Refrigeration effect is attained at a cold mass fraction of 80%. It is also observed that the cooling effect produced by the vortex tube depends on properties of the gas, molecular weight and specific heat ratio. The vortex tubes perform better with carbon dioxide compared to air and nitrogen owing to its high molecular weight and low specific heat ratio [9].

REFERENCES

[1] M. Yilmaz, M. Kaya, S. Karagoz, S. Erdogan, A review on design criteria for vortex tubes, Heat Mass Transfer 45 (2009) 613–632.
[2] Y. Xue, M. Arjomandi, R. Kelso, A critical review of temperature separation in a vortex
[3]. Takahama, H., Soga, N., 1965. Studies on vortex tubes report.
Trans. Japan Soc. Mech. Eng. 31, 787–794 .

[4] M.H. Saidi, M.R. Allaf Yazdi, Exergy model of a vortex tube system with experimental results, Energy 24 (1999) 625–632.

[5]. M.H. Saidi, M.S. Valipour, Experimental modeling of vortex tube refrigerator, Appl. Therm. Eng. 23 (2003) 1971–1980.

[6]. Eiamsa-ard, Experimental investigation of energy separation in a counter-flowRanque–Hilsch vortex tube with multiple inlet snail entries, Int. Commun. HeatMass Transfer 37 (2010) 637–643.

[7]. O. Aydin, B. Markal, M. Avci, A new vortex generator geometry for a counterflow Ranque–Hilsch vortex tube, Appl. Therm. Eng. 30 (2010) 2505–2511.

[8]. B. Markal, O. Aydin, M. Avci, An experimental study on the effect of the valve angle of counter-flow Ranque–Hilsch vortex tubes on thermal energy separation, Exp. Thermal Fluid Sci. 34 (2010) 966–971.
[9]. Experimental investigation of vortex tube using natural substances N. Agrawal
S.S. Naik, Y.P. Gawale .
[10]. C.U. Linderstrøm-Lang, Studies on Transport of Mass and Energy in the Vortex Tubes: the Significance of the secondary Flow and Its Interaction with the
Tangential Velocity Distribution, Risb Report No. 248, 1971. Exp. Thermal Fluid Sci. 34 (2010) 1367–1374.

[11]. B. Markal, O. Aydin, M. Avci, An experimental study on the effect of the valve angle of counter-flow Ranque–Hilsch vortex tubes on thermal energy separation, Exp. Thermal Fluid Sci. 34 (2010) 966–971.

[12] Smith Eiamsa-ard, Pongjet Promvonge, Review of Ranque–Hilsch effects in vortex tubes, Renew. Sust. Energ. Rev. 12 (2008) 1822–1842.
[13] O. Aydin,M. Baki, An experimental study on the design parameters of a counterflow vortex tube, Energy 31 (2006) 2763–2772.
[14] J. Sarkar, Review on cycle modifications of transcritical CO2 refrigeration and heat pump systems, J. Adv. Res. Mech. Eng. 1 (2010) 22–29.
[15]. Investigation of the energy separation effect and flow mechanism inside a vortex tube Xingwei Liu, Zhongliang Liu.
[16]. O. Redlich, J.N.S. Kwong, On the thermodynamics of solutions. V. An equation of state. Fugacities gaseous solutions, Chem. Rev. 44 (1949) 233e244.
[17]. CFD analysis and experimental investigations towards optimizing the parameters of Ranque–Hilsch vortex tube , Upendra Behera, P.J. Paul,
S. Kasthurirengan, R. Karunanithi, S.N. Ram, K. Dinesh, S. Jacob.
[18]. Experimental investigation of vortex tube using natural substances☆
N. Agrawal, S.S. Naik, Y.P. Gawale.
 [19] .O. Redlich, J.N.S. Kwong, On the thermodynamics of solutions. V. An equation of state. Fugacities gaseous solutions, Chem. Rev. 44 (1949) 233e244.
[20].Saidi, M.H., Allaf Yazdi, M.R., 1999. Exergy model of a vortex tube
system with experimental results. Energy 24, 625e632.

[21].   G.J. Ranque, Experiences sur la detente giratoire avec productions simultanes   d_un echappement d_air chaud et d_un echappement d_air froid, J. Phys. Radium 4 (7) (1933) 112–114.

[22] R. Hilsch, The use of the expansion of gases in a centrifugal field as cooling process, Rev. Sci. Instrum. 18 (2) (1947) 108–113.

[23] R.G. Deissler, M. Perlmutter, Analysis of the flow and energy separation in a turbulent vortex, Int. J. Heat Mass Transfer 1 (1960) 173–191.

[24] M. Kurosaka, Acoustic streaming in swirl flow and the Ranque–Hilsch (vortex-tube) effect, J. Fluid Mech. 124 (1982) 139–172.

[25] B. Ahlborn, J.U. Keller, R. Staudt, G. Treitz, E. Rebhan, Limits of temperature separation in a vortex tube, Phys. D: Appl. Phys. 27 (1994) 480–488.

[26] T.T. Cockerill, Thermodynamics and Fluid Mechanics of a Ranque Hilsch Vortex Tube, Masters Thesis, University of Cambridge, England, 1995.

[27] A.F. Gutsol, The Ranque effect, Phys.—Uspekhi 40 (6) (1997) 639–658.

[28] B.K. Ahlborn, J.U. Keller, E. Rebhan, The heat pump in a vortex tube, J. Non-Equilib. Thermodyn. 23 (2) (1998) 159–165.